Role of the C−H Stretch Mode Excitation in the Dynamics of the Cl + CHD_3 Reaction: A Quasi-classical Trajectory Calculation

J. Espinosa-García†

Departamento de Química Física, Universidad de Extremadura, 06071 Badajoz, Spain

Received: May 9, 2007; In Final Form: July 30, 2007

To analyze the effect of the C−H stretch mode excitation on the dynamics of the Cl + CHD_3 gas-phase abstraction reaction, an exhaustive state-to-state dynamics study was performed. This reaction can evolve along two channels: H-abstraction, CD_3 + ClH, and D-abstraction, CHD_2 + ClD. On an analytical potential energy surface constructed previously by our group, named PES-2005, quasi-classical trajectory calculations were performed at a collision energy of 0.18 eV, including corrections to avoid zero-point energy leakage along the trajectories. First, strong coupling between different vibrational modes in the entry valley was observed; i.e., the reaction is vibrationally nonadiabatic. Second, for the ground-state $CHD_3(\nu=0)$ reaction, the diatomic fragments appeared in their ground states, and the H- and D-abstraction reactions showed similar reactivities. However, when the reactivity per atom is considered, the H is three times more reactive than the D atom. Third, when the C−H stretch mode is excited by one quantum, $CHD_3(\nu_1=1)$, the H-abstraction is strongly favored, and the C−H stretch excitation is maintained in the product $CHD_2(\nu_1=1)$ + ClD channel; i.e., the reaction shows mode selectivity, reproducing the experimental evidence, and also the reactivity of the vibrational ground state is increased, in agreement with experiment. Fourth, the state-to-state angular distributions of the CD_3 and CHD_2 products showed the products to be practically sideways for the reactant ground state, while the C−H excitation yielded a more forward scattering, reproducing the experimental data. The role of the zero-point energy correction was also analyzed, and we find that the dynamics results are very sensitive on how the ZPE issue is treated. Finally, a comparison is made with the similar H + $CHD_3(\nu_1=0,1)$ and Cl + $CH_4(\nu_1=0,1)$ reactions.

1. Introduction

Recently our group has begun a series of studies focused on the theoretical analysis of mode- and bond-selective chemistry in polyatomic systems, an exciting field of research initiated by the pioneering experimental studies of Zare and co-workers[1−3] and Crim and co-workers.[4−6] Those studies analyzed the effects of both reactant stretching and bending excitations on the dynamics of polyatomic reactions and represent a theoretical and experimental challenge.

In a first contribution of this series,[7] we analyzed the reaction of hydrogen atoms with trideuteromethane in its vibrational ground state and the C−H stretch mode excited, which can evolve by two channels, H- and D-abstraction:

$$\mathrm{H} + \mathrm{CHD_3}(\nu_1=0,1) \rightarrow \mathrm{CD_3}(\nu) + \mathrm{H_2}(\nu')$$
$$\rightarrow \mathrm{CHD_2}(\nu) + \mathrm{HD}(\nu')$$

On the basis of an analytical potential energy surface for the CH_5 system previously constructed by our group[8] (PES-2002), we performed quasi-classical trajectory (QCT) calculations at a collision energy of 1.53 eV and compared the theoretical results with experimental information by Camden et al.[9] and theoretical data by Xie and Bowman.[10] We obtained the following conclusions. First, when the H atom approaches the CHD_3, one observes no transfer of energy in the first steps for this reaction, suggesting that the intramolecular vibrational redistribution will be small or negligible. Once the reactive collision occurs, the energy flows between different vibrational modes, suggesting that the reaction is vibrationally nonadiabatic. Second, in the ground-state $CHD_3(\nu=0)$ reaction, the D-abstraction is favored by a factor of 2. Third, the C−H stretch mode excitation enhances the reactivity for both channels, by a factor of ≈3 for the H-abstraction and ≈2 for the D-abstraction. Finally, the C−H stretch mode excitation is maintained in the $CHD_2(\nu_1=1)$ product for channel 2, suggesting mode selectivity. In sum, the QCT calculations reproduce the experimental evidence (always qualitatively and sometimes even quantitatively), which lends confidence to the PES-2002 and the method used.

Following this line, the present paper is an exhaustive analysis of the dynamics of the similar Cl + $CHD_3(\nu_1=0,1)$ reaction, both in its vibrational ground state and with the C−H stretch mode excited by one quantum. Experimentally, this reaction has been widely studied,[9,11,12] but there have apparently been no theoretical studies. As in the earlier case with hydrogen atoms, this reaction can evolve by two channels, H- and D-abstraction,

$$\mathrm{Cl} + \mathrm{CHD_3}(\nu_1=0,1) \rightarrow \mathrm{CD_3}(\nu) + \mathrm{ClH}(\nu')$$
$$\rightarrow \mathrm{CHD_2}(\nu) + \mathrm{ClD}(\nu')$$

Simpson et al.[11] for the Cl + $CHD_3(\nu_1=1)$ reaction reported state distributions and angular distributions for the ClH fragment. Later, that same laboratory[9] studied the reaction of Cl atoms with $CHD_3(\nu_1=0,1,2)$, finding that the ground-state reaction produces methyl fragments in their ground states only, CD_3-

† E-mail: joaquin@unex.es.

10.1021/jp073549u CCC: $37.00
Published on Web 09/08/2007

(ν=0) and CHD_2(ν=0), and that the H-abstraction reaction is more favored than for the similar H + CHD_3 reaction. When the C−H stretch mode is excited by one quantum, the H-abstraction is strongly favored, and the reaction presents mode selectivity, a feature similar to that of the H + CHD_3 reaction. Recently, Liu and co-workers[12] used a time-sliced velocity imaging technique to obtain information on the product pairs, CD_3(ν) + ClH(ν), although only for the H-channel. They concluded that the state-correlated findings were qualitatively but not quantitatively in line with previous results.[9,11] Thus, for instance, while Camden et al.[9] reported qualitatively that the C−H stretch mode excitation enhances the reactivity with respect to the ground-state reaction, Liu and co-workers[12] quantified this ratio at 5.8 ± 2.8.

To shed more light on the role of the C−H stretch excitation, the present work describes an exhaustive state-to-state dynamics study of the Cl + CHD_3(ν_1=0,1) reaction using QCT calculations on an analytical potential energy surface previously constructed by our group, named PES-2005.[13] The paper is structured as follows: Section 2 briefly outlines the potential energy surface and the computational details. The QCT dynamics results are presented in section 3 and compared with experimental results. Sections 4 and 5 are devoted to a comparison with the similar H + CHD_3(ν_1=0,1), and Cl + CH_4(ν_1=0,1) reactions, respectively. Finally, section 6 presents the conclusions.

2. Potential Energy Surface and Computational Details

In 2005 our group constructed a new PES for the gas-phase Cl + CH_4 → HCl + CH_3 polyatomic reaction,[13] which is symmetric with respect to the permutation of the methane hydrogen atoms, a feature that is especially interesting for dynamics calculations. The functional form was developed in that work, and therefore will not be repeated here. Basically, it consists of four LEP-type (London−Eyring−Polanyi) stretching terms (str), augmented by out-of-plane (op) bending and valence (val) bending terms. In the calibration process we fitted some of the parameters of the analytical PES in order to reproduce the variation of the experimental thermal forward rate constants with temperature.

Because of the great quantity of experimental information available for this reaction, this PES-2005 was subjected to a great variety of tests, both kinetic and dynamic. Thus, from the kinetics point of view, first the forward and reverse thermal rate constants calculated using variational transition-state theory (VTST) with semiclassical transmission coefficients were found to agree with experimental measurements, reproducing the curvature of the Arrhenius plot. Second, we found excellent agreement of the very sensitive $^{12}CH_4/^{13}CH_4$ kinetic isotope effects (KIEs), good agreement for deuterium KIEs, and moderate agreement for the overall deuterated CD_4 KIE. Note that these KIEs constitute a very sensitive test of features of the new surface, such as barrier height and width, zero-point energy, and tunneling effect.

From the dynamics point of view, an extensive study employing QCT calculations was also performed on this surface, dealing with both ground-state and asymmetric vibrationally excited C−H stretching methane. First, we found that excitation of the ν_3 mode enhances the forward rate constants by a factor of 14, as compared to the experimental value 30 ± 15.[11] Second, our QCT calculations give HCl rotational distributions slightly hotter than experiments by 1 or 2 units of j', although they correctly describe the experimental trend of decreasing HCl product rotation excitation in going from HCl(v'=0) to HCl(v'=1) for the CH_4(ν_3=1) reaction. Third, the state-specific scattering distributions present qualitative agreement with experiment. In sum, this reasonable agreement with a great variety of kinetics and dynamics results lends confidence to this PES-2005 polyatomic surface, although there are some differences which may be due to the PES, but also to the known limitations of the QCT method (especially the treatment of the vibrational zero-point energy (ZPE), i.e., the ZPE breakdown problem).

The QCT calculations[14−16] were carried out using the VENUS96 code,[17] customized to incorporate our analytical PES. Moreover, two modifications were included to compute the average energy in each normal mode to obtain information first on the temporal evolution of this energy through the first steps of the reaction, which is related to the quantum mechanical intramolecular vibrational redistribution (IVR) in the entry valley, and second on the CD_3 and CHD_2 co-product vibrational distribution depending on the exit valley. Since VENUS96 freely rotates the molecules along the trajectories, the normal mode energy calculation is preceded by a rotation of the molecule in order to maintain the orientation of the optimized geometry of the respective products depending on the channel for which the normal mode analysis was performed. Once this is done, a projection of the displacement and momentum matrices on the respective normal mode space allows one to compute the potential and kinetic energy, and therefore the total energy, for each normal mode.

To study the IVR in CHD_3 (note that our calculations are classical in nature, and therefore we use this nomenclature only for clarity), we performed batches of 500 nonreactive trajectories. The initial conditions were set so that we ensured that no reaction takes place during the trajectory. Each set of trajectories was run for the CHD_3 ground state and with a C−H stretch excitation by one quantum, and the energy for each normal mode was averaged for all trajectories in each case. The variation in each normal mode's average energy was taken as an indication of the internal flow of energy between normal modes in CHD_3. Note that this energy flow occurs before the collision with the Cl atom, so that it is not related to the mode−mode coupling along the reaction path (Coriolis-like terms) that we take as a qualitative indication of the energy flow when a reactive collision occurs.

To study the vibrational state of the CD_3 and CHD_2 products, the energy in each harmonic normal mode was computed for the last geometry (coordinates and momenta) on the reactive trajectories and averaged for all the reactive trajectories. Since the harmonic approximation was used for this calculation, one could expect the procedure to break down for highly excited states. However, because we are interested in the lowest CD_3 and CHD_2 vibrational states, we can assume that this method is accurate enough for the present purpose. This approach had been used in earlier papers by our group[7,18−20] with excellent results.

To compare experimental and theoretical QCT results, for each reaction considered in this work, namely, CHD_3 ground state and with the C−H stretch mode vibrationally excited, batches of 100 000 trajectories were calculated in which the impact parameter, b, was sampled by $b = b_{max}R^{1/2}$, with R being a random number in the interval [0,1]. The maximum value of the impact parameter calculated is 2.7 and 3.4 Å for the ground-state CHD_3(ν=0) reaction and C−H stretch mode excitation CHD_3(ν=1), respectively. The integration step was 0.01 fs, with an initial separation between the Cl atom and the CHD_3 molecule center of mass of 6.0 Å, and a rotational energy of

TABLE 1: Harmonic Vibrational Frequencies (cm^{-1}) with the PES-2005[a]

CHD_3	CD_3	CHD_2
3015 (ν_1) C−H sym stretch	2377 (ν_3) C−D asym stretch	3131 (ν_1) C−H sym stretch
2260 (ν_4) C−D asym stretch	2129 (ν_1) C−D sym stretch	2377 (ν_5) C−D asym stretch
2095 (ν_2) C−D sym stretch	912 (ν_4) deformation	2202 (ν_2) C−D sym stretch
1312 (ν_5) rock	457 (ν_2) umbrella	1136 (ν_6) C−H bend
1060 (ν_6) deformation		918 (ν_3) scissors
1045 (ν_3) umbrella		505 (ν_4) out-of-plane

[a] ClH, 3014; ClD, 2165 cm^{-1}.

300 K. To simulate the experimental conditions,[9] we considered a relative translational energy of 0.18 eV. The accuracy of the trajectory was checked by the conservation of total energy and total angular momentum.

A serious drawback of the QCT calculations is related to the question of how to handle the quantum mechanical ZPE problem in the classical mechanics simulation.[21−32] Many strategies have been proposed to correct for this quantum-dynamics effect (see, for instance, refs 21−25 and 28, and references therein), but no completely satisfactory alternatives have emerged. Here, we employed a pragmatic solution, the so-called passive method,[25] consisting of discarding all the reactive trajectories that lead, depending on the channel, to either a ClH (ClD) or a CD_3 (CHD_2) product with a vibrational energy below their respective ZPE. This we call histogram binning with double ZPE correction (HB-DZPE).

3. Results and Discussion

3.1. Nomenclature and Coupling of the Normal Modes. To clarify the nomenclature used in the text, we shall start by listing in Table 1 the vibration normal modes in reactants (CHD_3) and products (ClH and CD_3 for the first channel, and ClD and CHD_2 for the second) obtained with the PES-2005 surface.

For the first channel, we find that the C−H stretch mode, ν_1, is coupled to the reaction coordinate and evolves adiabatically to the ClH stretch mode, while the CHD_3 umbrella bending mode, ν_3, evolves adiabatically to the CD_3 product umbrella mode, ν_2. For the second channel, the C−D symmetric stretch mode, ν_2, is coupled to the reaction coordinate and evolves adiabatically to the ClD stretch mode, while the CHD_3 umbrella bending mode, ν_3, evolves adiabatically to the CHD_2 product out-of-plane mode, ν_4.

However, in previous work of our group[7,13,33,34] we found that this simple picture is incomplete and that coupling between the normal modes is significant, especially in the reactant valley, allowing some energy flow between the normal modes and leading to a vibrationally nonadiabatic picture. Following this idea, and in a similar way as in the earlier study of this series for the H + CHD_3 reaction,[7] we also performed an exhaustive analysis of the vibrational mode coupling for the title reaction, Cl + CHD_3, using two approaches: first, by calculating the temporal evolution of the energy available in different vibrational modes (equivalent to quantum mechanical IVR) using QCT calculations, and second, by calculating the coupling terms between vibrational modes, Bmm' (Coriolis-like terms).[35] The first approach can provide information about the energy flow between vibrational modes that takes place in the CHD_3 reactant preceding its collision with the Cl atom. The second approach gives information on the energy flow between the vibrational modes after the collision between the two reactants that will eventually evolve into the activated complex and then reach the products.

Figure 1 shows the temporal evolution of the energy available in different vibrational modes for the ground-state CHD_3 reactant (panel a) and after C−H stretch mode excitation by one quantum (panel b) averaged over all nonreactive trajectories. In both the CHD_3 ground state and excited C−H stretch mode the quasi-classical trajectory calculations show a flux of energy from the C−D symmetric stretch, ν_2 mode, to the doubly degenerate rock bending, ν_5 mode, although quantum-mechanically the energy transferred does not suffice to excite the ν_5 mode, and the molecule remains in its ground state. The effect of the C−H stretch excitation by one quantum (panel b) is mostly to shift its corresponding curve, and this mode will remain excited until CHD_3 collides with the Cl atom. Therefore, since the initial conditions were set so that no reaction takes place during the trajectory, no transfer of energy is observed before chlorine atom interacts with methane, and we conclude that the intramolecular vibrational redistribution will be small or negligible. This behavior agrees with the results found for the H + CHD_3 reaction using a very different PES, and disagrees with the experimentally based suggestion by Camden et al.[9] that the IVR will be more important in the present reaction.

Once the reactive collision occurs, the energy flow between modes can be monitored by the coupling terms Bmm′. Figure 2 shows the coupling matrix for the nine vibrational modes in CHD_3 along the reaction path for channels 1 and 2. In these plots the peaks indicate large coupling between the modes listed on the axes. In the first channel, Figure 2 (panel a), the coupling is especially important for the C−H stretching mode (ν_1) with

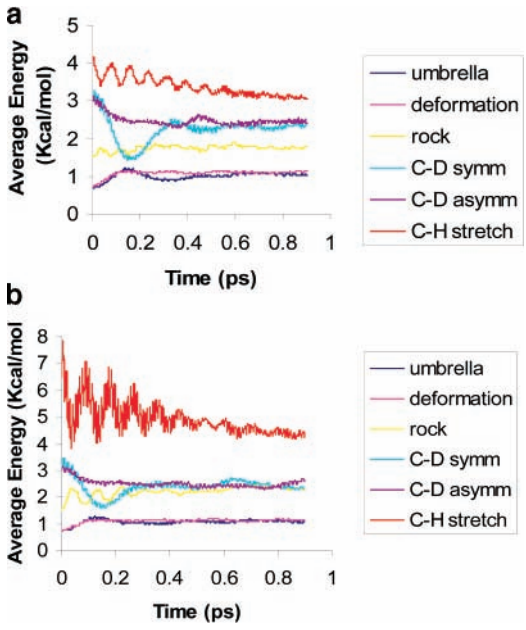

Figure 1. Average energy of each normal mode of CHD_3 from QCT calculations, as a function of time. Panel a shows the results for ground-state CHD_3, and panel b, for excitation of the C−H stretching mode by one quantum. The degenerate modes are represented by only one curve.

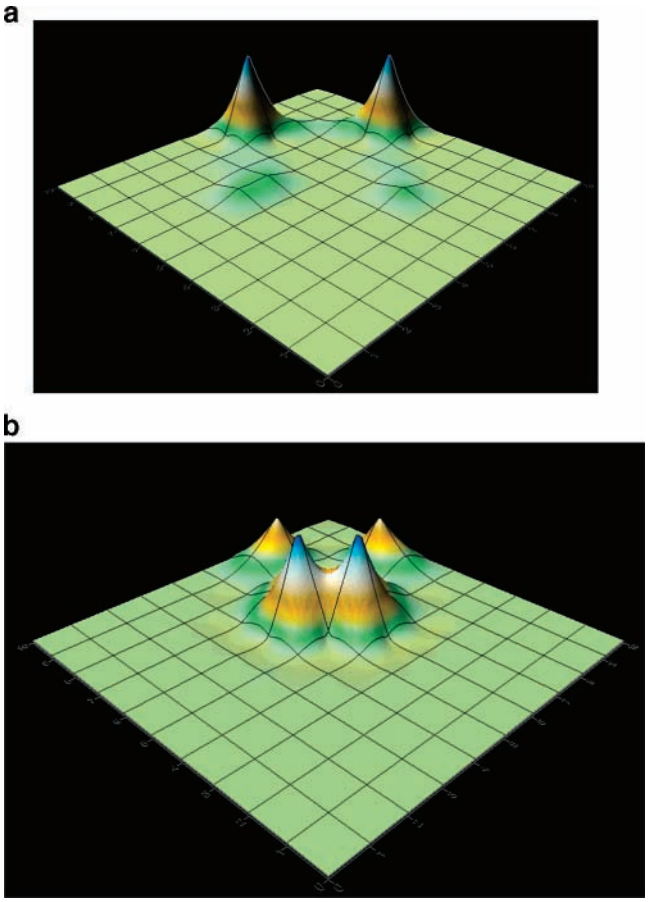

Figure 2. Coriolis-like Bmm′ coupling terms along the reaction path for the nine normal modes in CHD_3. The normal modes are numbered from higher to lower vibrational frequencies. Thus, mode 1 corresponds to ν_1, modes 2 and 3 correspond to ν_4, mode 4 to ν_2, modes 5 and 6 to ν_5, modes 7 and 8 to ν_6, and mode 9 to ν_3. Panel a shows the coupling terms for channel 1, CD_3 + ClH, while panel b shows the values computed for channel 2, CHD_2 + ClD.

the umbrella mode (ν_3), and to a lesser extent with the C−D symmetric stretch mode (ν_2). Other contributions from different couplings of bending modes are of less importance. In the second channel, Figure 2 (panel b), the coupling is especially important for the C−D symmetric stretch mode, ν_2, with the rock bending mode, ν_5 (mode 5), with the two deformation bending modes, ν_6 (modes 7,8), and with the umbrella mode, ν_3 (mode 9). The coupling for the deformation mode, ν_6 (mode 7) with the rock bending mode, ν_5 (mode 5), and the umbrella mode, ν_3 (mode 9), is also important. Therefore there is significant mode coupling, and the reaction does not preserve vibrational adiabaticity along the reaction path; i.e., the reaction is vibrationally nonadiabatic. Later, in section 4, this behavior will be compared with that for the similar H + CHD_3 reaction.[7]

3.2. Product Energy Partition. The QCT results for the ground-state and C−H vibrationally excited $CHD_3(\nu)$ reactant at a collision energy of 0.18 eV are listed in Table 2 for the two channels: P1, CD_3 + ClH; P2, CHD_2 + ClD. When the C−H stretch mode is excited by one quantum, in channel 1 the vibrational excitations of the CD_3 and ClH products increase, the first due to the coupling of the C−H mode (ν_1) with the C−D symmetric stretch mode along the reaction (see Figure 2) and the second indicating the adiabatic evolution from the C−H stretch mode in the reactants (which is coupled to the reaction coordinate; i.e., it is the reactive mode) to the Cl−H mode in the products. With respect to channel 2, the main change is in the vibrational excitation of the CHD_2 product, which increases

TABLE 2: Product Energy Partition (%)[a] at a Collision Energy of 0.18 eV for the Two Channels P1, CD_3 + ClH, and P2, CHD_2 + ClD

	$CHD_3(\nu=0)$		$CHD_3(\nu_1=1)$	
	P1	P2	P1	P2
$f_V(CD_3$ or $CHD_2)$[b]	7(50)[c]	11(50)	20(44)	36(66)
$f_R(CD_3$ or $CHD_2)$	17(4)	11(5)	9(5)	8(4)
f_V(ClH or ClD)	19(17)	19(18)	30(28)	20(13)
f_R(ClH or ClD)	12(11)	8(7)	13(9)	8(5)
f_T	45(18)	51(20)	29(14)	29(13)

[a] Calculated maximum error, ±1. Using the HB-DZPE correction, the total available energy in products is 4.4 and 3.6 kcal mol^{-1} for the P1 and P2 channels, respectively, in the $CHD_3(\nu=0)$ state and 13.0, and 12.2 kcal mol^{-1} for the same channels, but in the $CHD_3(\nu_1=1)$ state. [b] Values of the products depending on the channel. f_V, f_R, and f_T mean vibrational, rotational, and translational contributions, respectively. [c] Values in parentheses correspond to results taking into account all the reactive trajectories, i.e., without the ZPE restriction.

by a factor of >3 with respect to the ground-state reactant. These two last features indicate that the C−H stretch mode excitation to some extent preserves its character during the course of the reaction. Finally, it should be noted that a similar tendency was found for the H + CHD_3 reaction in a previous theoretical study,[7] but that unfortunately there is no direct experimental evidence for comparison.

To test the influence of the zero-point energy correction on this property, we also performed calculations considering all trajectories, i.e., without removing the trajectories with energies below the ZPE of the products. The results appear in Table 2, in parentheses, for the two channels. With respect to the HB-DZPE correction, the $CD_3(CHD_2)$ internal energy increases, while the translational energy diminishes. Therefore, the results are very sensitive to the ZPE criterion chosen, and obviously, this will influence other dynamics properties.

3.3. State-to-State Reaction Cross-Section. The state-to-state QCT reaction cross-sections, σ_R, at a collision energy of 0.18 eV for the two channels P1 and P2 are listed in Table 3.

The ground-state reaction, Cl + $CHD_3(\nu=0)$, produces exclusively diatomic molecules in their ground states, ClH($\nu=0$) and ClD($\nu=0$), and methyl fragments vibrationally excited in the umbrella mode: for $CD_3(\nu_2=1,2)$, 29%, and for CHD_2-($\nu_4=1,2$), 83%, of the total reactivity for channels 1 and 2, respectively. These values are vibrationally more excited than the experimental report[9] which showed that the methyl fragments are obtained in their vibrational ground state, but they are similar to those obtained in a previous QCT study of the H + CHD_3 reaction[7] using a very different PES. Therefore, the difference with experiment in the present reaction may be due to the known quantum limitations of the QCT method.

When the C−H stretch mode is excited by one quantum, a larger number of product paths are opened. First, the diatomic molecules appear mainly in their ground states, although not exclusively: for ClH($\nu=0$), 62%, and for ClD($\nu=0$), 71% of the total reactivity, for channels 1 and 2, respectively. For channel 1, Cl + $CHD_3(\nu_1=1) \rightarrow CD_3(\nu_2=0,1,2)$ + ClH, the CD_3 product appears mainly in its ground state, 82%, with a small fraction of umbrella excitation, 18%. This result reproduces the experimental observation.[9] Channel 2, Cl + CHD_3-($\nu_1=1$) → $CHD_2(\nu_4=0,1,2)$ + ClD, leads mainly also to methyl fragments in their ground states, although the contributions of the excitation of the out-of-plane, $CHD_2(\nu_4)$, and of the C−H stretch mode, $CHD_2(\nu_1)$, are important.

The reaction cross-section channel ratios, σ_1/σ_2, are 1.02 and 2.49 for $CHD_3(\nu_1=0)$ and $CHD_3(\nu_1=1)$, respectively. Thus, for the ground-state CHD_3 reaction, there is no clear preference

TABLE 3: State-to-State Reaction Cross-Section, σ_R (Å^2), at a Collision Energy of 0.18 eV

reactant state	product states	σ_R (Å^2)	percentage[a]
	$CHD_3(\nu_1=0)$ Reactant Ground State		
$CHD_3(\nu_1=0)$	$CD_3(\nu_2=0)$ + ClH(ν=0)	0.030	71
	$CD_3(\nu_2=1,2)$ + ClH(ν=0)	0.012	29
		0.042 (σ_1°)	
$CHD_3(\nu_1=0)$	$CHD_2(\nu_4=0)$ + ClD(ν=0)	0.007	17
	$CHD_2(\nu_4=1,2)$ + ClD(ν=0)	0.034	83
		0.041 (σ_2°)	
	$CHD_3(\nu_1=1)$ Reactant C−H Stretch Mode Excitation		
$CHD_3(\nu_1=1)$	$CD_3(\nu_2=0)$ + ClH(ν=0)	0.293	51
	$CD_3(\nu_2=0)$ + ClH(ν=1)	0.181	31
	$CD_3(\nu_2=1,2)$ + ClH(ν=0)	0.066	11
	$CD_3(\nu_2=1,2)$ + ClH(ν=1)	0.037	7
		0.577 ($\sigma_1^\ddagger$)	
$CHD_3(\nu_1=1)$	$CHD_2(\nu_4=0)$ + ClD(ν=0)	0.077	33
	$CHD_2(\nu_4=0)$ + ClD(ν=1)	0.030	13
	$CHD_2(\nu_4=1,2)$ + ClD(ν=0)	0.089	38
	$CHD_2(\nu_4=1,2)$ + ClD(ν=1)	0.036	16
		0.232 ($\sigma_2^\ddagger$)	
$CHD_3(\nu_1=1)$	$CHD_2(\nu_1=0)$ + ClD(ν=0)	0.140	60
	$CHD_2(\nu_1=0)$ + ClD(ν=1)	0.059	26
	$CHD_2(\nu_1=1)$ + ClD(ν=0)	0.026	11
	$CHD_2(\nu_1=1)$ + ClD(ν=1)	0.007	3
		0.232 ($\sigma_2^\ddagger$)	

[a] Percentage of the total reaction cross-section for each channel. In the last reaction, $CHD_3(\nu_1=1)$ + H, channel 2, we have separated the contributions for each CHD_2 vibrational state, ν_4 and ν_1, to avoid double counting the HD contributions, so that the total reaction cross (0.232) is the same for the two cases.

shown for the H- or D-abstraction, although the H/D ratio is greater than for the similar H + $CHD_3(\nu_1=0)$ reaction,[7] in agreement with experiment.[9] For the $CHD_3(\nu_1=1)$ vibrationally excited reaction, the H-abstraction, channel 1, is clearly dominant, again in agreement with experiment.

To better compare the results, we consider the number of H and D atoms that can be transferred from CHD_3, i.e., the integral cross-section per atom. Then, the comparison of the integral cross-section per atom shows that H is 3.1 times more reactive than D, for the ground-state $CHD_3(\nu_1=0)$, and 7.5 times more reactive for the excited-state $CHD_3(\nu_1=1)$. So, it becomes evident that the H-atom transfer is clearly favored over the D-atom transfer, and this behavior is enhanced by vibrational excitation of the C−H stretch mode in CHD_3.

The vibrational enhancement factor, $\sigma^\ddagger/\sigma^\circ$, is 13.7 and 5.6 for channels 1 and 2, respectively. While the second value has not been experimentally reported, the first value agrees with the qualitative experimental information of Camden et al.,[9] $\sigma_1^\ddagger\sigma_1^\circ > 1$, and with the recent experimental study of Yan et al.,[12] 5.8 ± 2.8, although our value is greater.

Recently, Liu and co-workers[36] deepened this issue, analyzing whether vibrational excitation is more effective in driving the Cl + $CHD_3 \rightarrow CD_3$ + ClH reaction (channel 1 in the present paper) than an equivalent amount of translational energy. These authors, unexpectedly, observed that the C−H stretch excitation is no more effective than translation.

The vibrational branching ratio for the following paths in channel 1,

$$\mathrm{Cl} + \mathrm{CHD_3}(\nu_1=1) \rightarrow \mathrm{CD_3}(\nu=0) + \mathrm{ClH}(\nu=0)$$
$$\rightarrow \mathrm{CD_3}(\nu=0) + \mathrm{ClH}(\nu=1)$$

ClH(ν=1)/ClH(ν=0), is 0.60. While Simpson et al.[11] reported a value of 0.22, the more recent study of Yan et al.[12] reported a value of 0.67 ± 0.21, in agreement with the present QCT calculations.

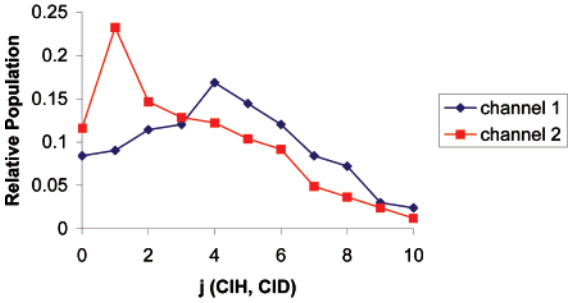

Figure 3. Rotational populations for the Cl + $CHD_3(\nu=0)$ ground-state reaction at a collision energy of 0.18 eV for the following: H-abstraction, channel 1, which leads to the CD_3 + ClH(ν=0) products; and D-abstraction, channel 2, which leads to the CHD_2 + ClD(ν=0) products. The distributions are normalized so that the area under the common levels is the same.

Finally, the influence of the ZPE correction is analyzed. When all trajectories are considered, i.e., without removing the trajectories with energies below the products's ZPE, the reaction cross-sections are as follows: $\sigma_1^\circ = 0.219$, $\sigma_2^\circ = 0.880$, $\sigma_1^\ddagger = 1.548$, and $\sigma_2^\ddagger = 0.472$ Å.^{2} Clearly, the reactivity increases strongly for all cases, and the branching ratios change. Therefore, the results are very sensitive to the ZPE criterion chosen.

Before finishing this section, we consider some concerns about the uncertainties in the calculations. In general, due to the large number of trajectories that ran in the calculations, we assume that the statistics are adequate, and the uncertainties, small (see, for instance, Table 2). However, because of the large number of paths opened for the title reaction, especially when vibrational excitations are considered (see Table 3), the uncertainties will increase for the paths where the reactivity diminishes, for instance, for the Cl + $CHD_3(\nu_1=0) \rightarrow CD_3(\nu_2=1,2)$ + ClH(ν=0), or Cl + $CHD_3(\nu_1=0) \rightarrow CHD_2(\nu_4=0)$ + ClD(ν=0) channels, where the reaction cross-sections are very small, 0.012 and 0.007 Å^2, respectively.

3.4. Rovibrational Distributions of the Bimolecular Products, ClH and ClD. As was noted earlier, the ground-state Cl + $CHD_3(\nu=0)$ reaction produces exclusively ClH(ν=0) and ClD(ν=0), i.e., diatomic fragments in their ground states. The rotational distributions are shown in Figure 3 for channels 1 and 2. While that of ClH peaks at $j = 4$, the ClD distribution is colder ($j = 1$). Clearly, this behavior is related to the rotational contributions, f_R, of the product energy partition seen in section 3.2. The comparison of the f_R shows that ClH(ν=0) in channel 1 is rotationally hotter than ClD(ν=0) in channel 2. Unfortunately, there is no experimental information for comparison.

Figure 4 plots the ClH(ν) and ClD(ν) rotational distributions for channels 1 (panel a) and 2 (panel b) when the C−H stretch mode is excited by one quantum. In general, both distributions have a longer tail than those of the ground-state $CHD_3(\nu=0)$ reaction. For channel 1, the only one with experimental data for comparison,[11] the ClH(ν) rotational distribution is colder when the vibrational state of ClH is hotter, with the j number peaking at 1 for ClH(ν=1), reproducing the experimental data. For channel 2, both the ClD(ν=0) and the ClD(ν=1) give cold rotational distributions, peaking at $j = 2$ and $j = 1$, respectively. Unfortunately, there is no experimental information for comparison.

3.5. Scattering Distributions of the CD_3 Polyatomic Products. The differential cross-section, DCS, is a key dynamic property, which is particularly helpful to reflect the accuracy of the theoretical dynamic approach used. Although the results, of course, also depend on the quality of the PES, it is harder to

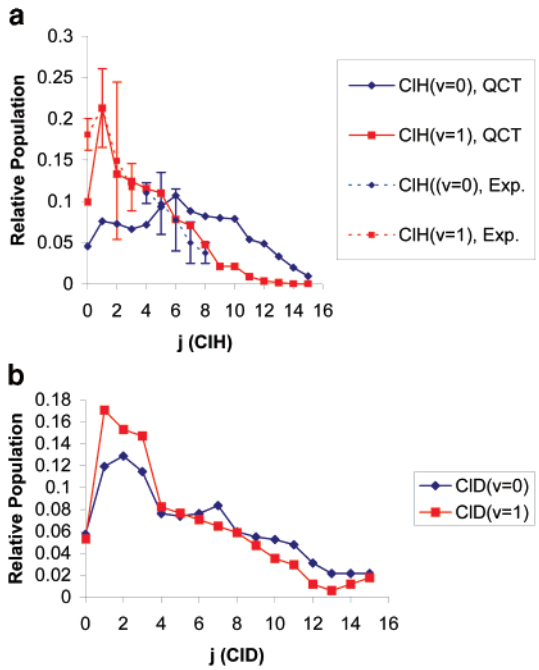

Figure 4. Rotational populations for the reaction with the C−H stretch mode excited by one quantum, Cl + $CHD_3(\nu_1=1)$ at a collision energy of 0.18 eV. Panel a corresponds to the H-abstraction, channel 1, which leads to the CD_3 + ClH(ν=0,1) products. Solid lines are our QCT results. Dashed lines with the corresponding error bar are experimental values from ref 11. Note that the experimental values are read directly from Figure 5 of ref 11, where the range of values of j is partial: ClH(ν=0) over the range $j = 4-8$, and ClH(ν=1) over the range $j = 0-3$. Therefore, for a clear comparison theory/experiment, we have considered the same population for the highest j value in each case. Panel b corresponds to the D-abstraction, channel 2, which leads to the CHD_2 + ClD(ν=0,1) products. In each panel the distributions are normalized so that the area under the common levels is the same.

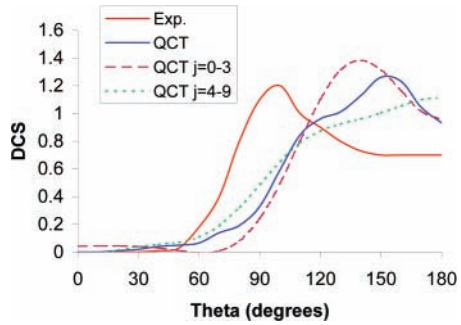

Figure 5. Product angular distribution at a collision energy of 0.18 eV for the main path Cl + $CHD_3(\nu=0) \rightarrow CD_3(\nu=0)$+ClH($\nu$=0) of channel 1, H-abstraction. The experimental data from ref 12 are also included for comparison. The distributions are normalized so that the area under the common levels is the same.

reproduce differential cross-sections than integral cross-sections in dynamic calculations.

The CD_3 product scattering with respect to the CHD_3 incident reactant (measured as the relative differential cross-section, DCS) for channel 1 is plotted in Figure 5 for the $CHD_3(\nu=0)$ ground-state reaction, together with the experimental data/values for comparison.[12] Experimentally it was found that, for the ground-state reaction, ClH(ν=0) + $CD_3(\nu=0)$, the angular distribution is predominantly sideways-peaked, with some backward contribution. The QCT results reproduce this behavior, although they are slightly more backward. However, in an earlier study on the H + CD_4 reaction[37] we observed that the rotational number of the diatomic molecule, j(HD), greatly influences the

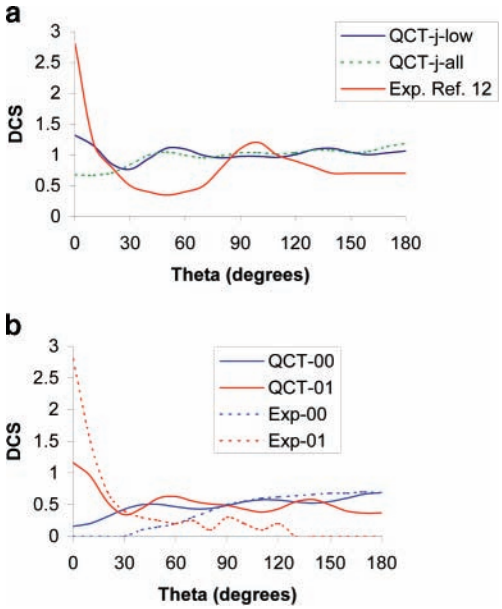

Figure 6. Product angular distribution at a collision energy of 0.18 eV for the reaction with the C−H stretch mode excited by one quantum, Cl + $CHD_3(\nu_1=1)$, for channel 1, H-abstraction. Panel a corresponds to the main path Cl + $CHD_3(\nu_1=1) \rightarrow CD_3(\nu=0)$ + ClH(ν=0,1). Panel b corresponds to the different contributions from the ClH product, ClH(ν=0) and ClH(ν=1). The distributions are normalized so that the area under the common levels is the same. The nomenclature "00" corresponds to the $CD_3(\nu=0)$ + ClH(ν=0) state, and the "01", to the $CD_3(\nu=0)$ + ClH(ν=1) state.

scattering, and the experimental angular distribution is reproduced when only the lowest j(HD) rotational numbers are considered. This behavior was explained by the known limitations of the traditional histogram binning procedure used in the QCT method, which gives artificial tails extending to very high rotational levels.[38−42] To analyze this effect in the present reaction, Figure 5 includes a plot of the QCT results at low j(ClH), 0−3, and high j(ClH), 4−9, values. In this latter case, the angular distribution is clearly backward, while the lower j(ClH) values are closer to the experimental evidence.

The C−H stretch mode excitation sharply changes the angular distribution, suggesting a mode-selective reaction dynamics (Figure 6, Panel a). Experimentally, Yan et al.[12] found that the angular distribution is sideways and strongly forward. The QCT results show a change of the angular distribution in line with experiment, but it is practically isotropic, where the forward peak is really small. Note that, in accordance with the comments above on the role played by the rotational number j(ClH) in the angular distribution, in this case only the lower j(ClH) values were considered. When all the j(ClH) values were considered, the behavior was more isotropic and the forward peak disappeared (dashed line in Figure 6a). Again, this is a reflection of the influence of the rotational number on the angular distribution.

The state-to-state angular distributions for channel 1 have been also reported experimentally.[12] This experimental information together with the QCT results are plotted in Figure 6, panel b, for the following paths:

$$\text{Cl} + \text{CHD}_3(\nu_1=1) \rightarrow \text{CD}_3(\nu=0) + \text{ClH}(\nu=0); \quad \text{path 00}$$

$$\rightarrow \text{CD}_3(\nu=0) + \text{ClH}(\nu=1); \quad \text{path 01}$$

Experimentally, while path 00 is mainly back- and sideways-scattered, path 01 is predominantly forward. The QCT results reproduce this behavior, although path 01 is less forward-scattered.

TABLE 4: Some Energy and Kinetics Parameters[a] for the PES-2002 and PES-2005 Surfaces of H + CH_4 and Cl + CH_4, Respectively

	ΔH_R(0K)	$\Delta E^{\ddagger}$	$\Delta H^{\ddagger}$(0K)	k(298K)	E_a
PES-2002, H + CHD_3 Reaction[b]					
channel 1	0.60	12.9	12.01	4.11×10^{-19}	12.06
channel 2	1.38	12.9	13.07	5.02×10^{-20}	13.08
PES-2005, Cl + CHD_3 Reaction[c]					
channel 1	1.68	7.6	2.62	3.40×10^{-14}	3.86
channel 2	2.04	7.6	3.76	1.14×10^{-14}	4.76

[a] ΔH_R(0K), enthalpy of reaction at 0 K; $\Delta E^{\ddagger}$, classical barrier height; $\Delta H^{\ddagger}$(0K), conventional transition-state enthalpy of activation at 0 K; k(298K), rate constant at 298 K; E_a, activation energy (400−900 K for the H + CHD_3 reaction and 300−500 K for the Cl + CHD_3 reaction). Energy values in kcal/mol, and rate constants in cm^3 $molecule^{-1}$ s^{-1}. [b] Channel 1, CD_3 + H_2; channel 2, CHD_2 + HD. [c] Channel 1, CD_3 + ClH; channel 2, CHD_2 + ClD.

4. Comparison of the H and Cl Reactions with CHD_3(ν_1=0,1)

As was noted in the Introduction, in a previous study[7] we analyzed the dynamics of the similar H + CHD_3(ν_1=0,1) reaction, using QCT calculations on the PES-2002 previously constructed by our group[8] at a collision energy of 1.53 eV. In this section, the dynamics of this reaction will be compared with the similar Cl + CHD_3(ν_1=0,1) reaction studied in depth in the foregoing sections also using QCT calculations but on a different surface, PES-2005,[13] at a collision energy of 0.18 eV. For the convenience of the reader, Table 4 summarizes some important features of the two surfaces, PES-2002 and PES-2005, and some kinetic data that may be useful for a clearer comparison of the H and Cl reactions with CHD_3.

In the ground-state CHD_3(ν=0) process, the two reactions present similar behavior, both in the state-to-state reaction cross-section,

	H, %	Cl, %
Cl/H + CHD_3(ν=0) → CD_3(ν=0) + Cl/H−H	66	71
→ CHD_2(ν=0) + Cl/H−D	25	17

and in the angular distribution, which is roughly sideways in both cases but with a slightly more backward tendency for the Cl reaction. The main difference between the two reactions is that while in the H reaction the diatomic products, H−H or H−D, appear with some vibrational excitation, 8−10% of the total reactivity, in the Cl reaction the diatomic products, Cl−H or Cl−D, appear in their ground states. Since the vibrational frequency is greater in the H case (H−H, 4406 and H−D, 3816 cm^{-1} versus Cl−H, 3014 and Cl−D, 2165 cm^{-1}), this greater vibrational excitation for the H reaction can be explained by the greater collision energy for the H reaction, 1.53 eV versus 0.18 eV, so that more energy is available for distribution.

When the C−H stretch mode is excited by one quantum, the state-to-state reaction cross-section is similar in both reactions for channel 1,

	H, %	Cl, %
Cl/H + CHD_3(ν_1=1) → CD_3(ν=0) + Cl/H−H	67	51
→ CHD_2(ν=0) + Cl/H−D	8	60
→ CHD_2(ν_1=1) + Cl/H−D	57	11

CD_3 + Cl/H−H, 67% versus 51% for the H and Cl reactions, respectively, but differs for channel 2, where the relative reactivity is inverted; i.e., while the Cl reaction gives mainly CHD_2(ν=0) in its ground state, 60%, the H-reaction gives mainly CHD_2(ν_1=1), 57%, suggesting that mode selectivity is more important in this latter case. Since both the H and Cl reactions show little or negligible intramolecular vibrational redistribution, this difference could be explained by the mode coupling in the entry valley once the Cl/H atom reacts with CHD_3. Thus, the H reaction is more vibrationally adiabatic than the Cl reaction. This can be seen in more detail by analyzing the Coriolis's terms for the two reactions (Cl/H). Consider first channel 1. For the H reaction the C−H stretch reactive mode is coupled to the C−D asymmetric and symmetric stretch modes, with small or negligible coupling between other modes. For the Cl reaction, the C−H stretch reactive mode is coupled to the C−D symmetric stretch mode and the umbrella mode, with noticeable coupling between other modes. For channel 2, while the H reaction presents small coupling between the C−D symmetric reactive mode and the rock bending mode, the Cl reaction shows a more complex situation, with strong coupling for the C−D symmetric reactive mode with the rock, with the deformation, and with the umbrella bending modes, and for the deformation bending with the rock and with umbrella bending modes. This more complex behavior shows that the Cl reaction has a more vibrationally nonadiabatic character than the similar H reaction.

The angular distribution is very similar in the two reactions (H/Cl), where the C−H stretch mode excitation yields a shift toward the more forward region in both reactions with respect to the ground-state CHD_3(ν=0) reaction.

5. Comparison of the Cl Reactions with CHD_3(ν_1=0,1) and CH_4(ν_1=0,1)

The foregoing sections have described a direct comparison with the previously studied H + CHD_3(ν_1=0,1) reaction,[7] focused on the influence of the C−H stretch mode excitation on the dynamics. However, this reaction is only formally similar to the title reaction, Cl + CHD_3(ν_1=0,1). For example, the kinematics and the shape of the PES for Cl + CHD_3 are very different from those for H + CHD_3 (reduced mass, 12.4 and 0.94 amu, respectively; see also Table 4). Moreover, the reaction conditions studied are also very different: collision energies of 0.18 and 1.53 eV, respectively.

Additional comparison with the Cl + CH_4(ν_1=0,1) reaction dynamics should be of interest, mainly regarding channel 1 (CD_3 + ClH), because the kinematics of Cl + CHD_3 and Cl + CH_4 are very similar, both reactions occur on the same PES, and the collision energies investigated are quite similar, 0.18 and 0.159 eV, respectively. This reaction has also been widely studied by our group.[13,33]

We begin by analyzing the reactant ground-state, CHD_3(ν_1=0) and CH_4(ν_1=0), processes, where the two reactions have similar behavior. The QCT reaction cross-sections, σ, for the Cl + CH_4(ν_1=0), and Cl + CHD_3(ν_1=0) are, respectively, 0.28 and 0.042 $Å^2$. A priori, one can thus say that chlorine atom is 6 times more reactive with CH_4 than with CHD_3. However, to better compare these results, one should consider the number of H atoms that can be transferred. The reactivity per atom is then similar in the two cases, only 1.5 times more reactive for the CH_4 reactant. This behavior can be explained by the difference in the maxima of the vibrationally adiabatic curves, 2.4 vs 2.6 kcal mol^{-1}, for the CH_4 and CHD_3, respectively.

In both reactions the population of the vibrationally excited ClH(ν=1) product is negligible, in agreement with experiment,[43] while the umbrella mode of the polyatomic product, CD_3(ν_2) and CH_3(ν_2), appears vibrationally excited, 29 and 44%, respectively. With respect to the angular distribution, we find

first a strong dependence with the rotational level of the diatomic product, ClH(v, j), and second, that the experimental results (predominantly sideways, with some backward contribution for both reactions)[12,44] are only reproduced when the lowest ClH(j) values are considered. As was noted above (section 3.5), this behavior can be explained by the known limitations of the QCT method resulting from its classical nature.

Next, we consider the C−H symmetric (ν_1) stretch mode excitation by one quantum. First, the vibrational excitation leads to a similar increase in the reactivity of both the $CH_4(\nu_1=1)$ and the $CHD_3(\nu_1=1)$ reactions, by factors of 16 and 14, respectively. Second, the vibrational branching ratios, ClH(ν=1)/ClH(ν=0), are 0.11 and 0.60 for the $CH_4(\nu_1=1)$ and $CHD_3(\nu_1=1)$ reactions, respectively. While the former clearly disagrees with the experimental values ($\approx$0.5),[1] the second agrees with the most recent study of Yan et al. (0.67 ± 0.21).[12] Since the same potential energy surface, and QCT method are used in both reactions, we do not have sufficient information here to explain the disagreement found for the Cl + $CH_4(\nu_1=1)$ reaction. Third, the C−H stretch mode excitation sharply changes the angular distribution for both reactions, $CH_4(\nu_1=1)$ and $CHD_3(\nu_1=1)$, with a clear tendency toward a more forward distribution, especially when the ClH(ν=1) product is analyzed. This is the expected behavior because the greater available energy opens the cone of acceptance, leading to larger impact parameters and thereby favoring the stripping over the rebound mechanism.

In sum, from this comparison between the Cl + $CH_4(\nu_1=0,1)$ and Cl + $CHD_3(\nu_1=0,1)$ reactions, it is evident that the two reactions present similar dynamics behavior, both in the reactant vibrational ground-state and when excited by one quantum.

6. Conclusions

With the aim of analyzing the effect of the C−H stretch mode excitation by one quantum in $CHD_3(\nu_1=0,1)$ on the dynamics of its reaction with chlorine atoms, exhaustive state-to-state QCT calculations were performed on an analytical potential energy surface previously constructed by our group (PES-2005). This is apparently the first theoretical study on this polyatomic system. This reaction can evolve along two channels, H- and D-abstraction (CD_3 + ClH and CHD_2 + ClD).

1. Before the collision between the reactants, no transfer of energy between vibrational modes is observed for this reaction, but once the reaction occurs, strong coupling between some vibrational modes is found, allowing the nonadiabatic flow of energy between modes. They therefore do not preserve their adiabatic character along the reaction path, i.e., the reaction is vibrationally nonadiabatic. This behavior has also been reported for the similar H + CHD_3 reaction, although to a lesser extent.

2. The C−H stretch mode excitation by one quantum increases the reactivity with respect to the vibrational ground state by factors of 13.7 for the H-abstraction (CD_3 + ClH) and 5.6 for the D-abstraction (CHD_2 + ClD). While the latter value has not been experimentally reported, the first value agrees with experimental evidence.

3. For channel 2, CHD_2 + ClD, the C−H excitation by one quantum in the reactants, $CHD_3(\nu_1=1)$, is maintained in the products, $CHD_2(\nu_1=1)$, indicating that the reaction shows mode selectivity. However, due to the larger coupling between modes for the Cl reaction, this mode selectivity is less pronounced than for the similar H + $CHD_3(\nu_1=1)$ reaction, 11% versus 57%.

4. For the CHD_3 reactant in its vibrational ground state, the CD_3 + ClH and CHD_2 + ClD channels yield predominantly sideways scattered CD_3. The C−H stretch mode excitation by one quantum leads to a shift toward forward scattering for both channels. These theoretical results reproduce the available experimental information and show behavior that is similar to that of the H + $CHD_3(\nu_1=1)$ reaction.

Acknowledgment. This work was partially supported by the Junta de Extremadura, Spain (Project No. 2PR04A001).

References and Notes

(1) Bechtel, H. A.; Camden, J. P.; Brown, D. J. A.; Zare, R. N. *J. Chem. Phys.* **2004**, *120*, 5096.
(2) Kim, Z. H.; Bechtel, H. A.; Camden, J. P.; Zare, R. N. *J. Chem. Phys.* **2005**, *122*, 084303.
(3) Camden, J. P.; Bechtel, H. A.; Brown, D. J. A.; Zare, R. N. *J. Chem. Phys.* **2005**, *123*, 134301.
(4) Yoon, S.; Henton, S.; Zirkovic, A. N.; Crim, F. F. *J. Chem. Phys.* **2002**, *116*, 10744.
(5) Yoon, S.; Holiday, R. J.; Crim, F. F. *J. Chem. Phys.* **2003**, *119*, 4755.
(6) Yoon, S.; Holiday, R. J.; Silbert, III, E. L.; Crim, F. F. *J. Chem. Phys.* **2003**, *119*, 9568.
(7) Espinosa-Garcia, J. *J. Phys. Chem. A* **2007**, *111*, 5792.
(8) Espinosa-García, J. *J. Chem. Phys.* **2002**, *116*, 10664.
(9) Camden, J. P.; Bechtekl, H. A.; Brown, D. J. A.; Zare, R. N. *J. Chem. Phys.* **2006**, *124*, 034311.
(10) Xie, Z.; Bowman, J. M. *Chem. Phys. Lett.* **2006**, *429*, 355.
(11) Simpson, W. R.; Rakitzis, T. P.; Kandel, S. A.; Orr-Ewing, A. J.; Zare, R. N. *J. Chem. Phys.* **1995**, *103*, 7313.
(12) Yan, S.; Wu, Y.-T.; Liu, K. *Phys. Chem. Chem. Phys.* **2007**, *9*, 250.
(13) Rangel, C.; Navarrete, M.; Corchado. J.C.; Espinosa-García, J. *J. Chem. Phys.* **2006**, *124*, 124306.
(14) Porter, R. N.; Raff, L. M. In *Dynamics of Molecular Collisions*, Part B; Miller, W. H., Ed.; Plenum Press: New York, 1976.
(15) Truhlar, D. G.; Muckerman, J. T. In Atom−Molecules Collision Theory; Bernstein, R. B., Ed.; Plenum Press: New York, 1979.
(16) Raff, L. M.; Thompson, D. L. In *Theory of Chemical Reaction Dynamics*, Vol. 3; Baer, M., Ed.; CRC Press: Boca Raton, FL, 1985.
(17) Hase, W. L.; Duchovic, R. J.; Hu, X.; Komornicki, A.; Lim, K. F.; Lu, D-h.; Peslherbe, G. H.; Swamy, K. N.; Van de Linde, S. R.; Varandas, A. J. C.; Wang, H.; Wolf, R. J. VENUS96: A General Chemical Dynamics Computer Program. *QCPE Bull.* **1996**, *16*, 43.
(18) Rangel, C.; Corchado, J. C.; Espinosa-García, J. *J. Phys. Chem. A* **2006**, *110*, 10375.
(19) Espinosa-García, J.; Bravo, J. L.; Rangel, C. *J. Phys. Chem. A* **2007**, *111*, 2761.
(20) Espinosa-García, J. *J. Phys. Chem. A* **2007**, *111*, 3497.
(21) Bowman, J. M.; Kuppermann, A. *J. Chem. Phys*. **1973**, *59*, 6524.
(22) Truhlar, D. G. *J. Phys. Chem*. **1979**, *83*, 18.
(23) Schatz, G. C. *J. Chem. Phys*. **1983**, *79*, 5386.
(24) Lu, D-h.; Hase, W. L. *J. Chem. Phys*. **1988**, *89*, 6723.
(25) Varandas, A. J. C. *Chem. Phys. Lett.* **1994**, *225*, 18.
(26) Ben-Nun, M.; Levine, R. D. *J. Chem. Phys*. **1996**, *105*, 8136.
(27) McCormack, D. A.; Lim, K. F. *Phys. Chem. Chem. Phys*. **1999**, *1*, 1.
(28) Stock, G.; Müller, U. *J. Chem. Phys.* **1999**, *111*, 65.
(29) Marques, J. M. C.; Martinez-Nuñez, E.; Fernandez-Ramos, A.; Vazquez, S. *J. Phys. Chem.* **2005**, *109*, 5415.
(30) Duchovic, R. J.; Parker, M. A. *J. Phys. Chem*. **2005**, *109*, 5883.
(31) Bonnet, L.; Rayez, J. C. *Chem. Phys. Lett.* **1997**, *183*, 277.
(32) Bonnet, L.; Rayez, J. C. *Chem. Phys. Lett.* **2004**, *397*, 106.
(33) Sanson, J.; Corchado, J. C.; Rangel, C.; Espinosa-Garcia, J. *J. Chem. Phys.* **2006**, *124*, 074312.
(34) Sanson, J.; Corchado, J. C.; Rangel, C.; Espinosa-Garcia, J. *J. Phys. Chem. A* **2006**, *110*, 9568.
(35) Miller, W. H.; Handy, N. C.; Adams, J. E. J. *Chem. Phys.* **1980**, *72*, 99.
(36) Yan, S.; Wu, Y.-T.; Zhang, B.; Yae, X.-F.; Liu, K. *Science* **2007**, *316*, 1723.
(37) Rangel, C.; Sanson, J.; Corchado, J. C.; Espinosa-Garcia, J.; Nyman, G. *J. Phys. Chem. A* **2006**, *110*, 10715.
(38) Wang, X.; Ben-Nun, M.; Levine, R.D. *Chem. Phys*. **1995**, *197*, 1.
(39) Troya, D.; Millan, J.; Baños, I.; Gonzalez, M. *J. Chem. Phys.* **2002**, *117*, 5730.
(40) Troya, D. *J. Chem. Phys*. **2005**, *123*, 214305.
(41) Castillo, J. F.; Aoiz, F. J.; Bañares, L.; Martinez-Nuñez, A.; Fernández-Ramos, A.; Vazquez, S. *J. Phys. Chem. A* **2005**, *109*, 8459.
(42) Troya, D.; Weiss, P. J. E. *J. Chem. Phys*. **2006**, 124, 074313.
(43) Simpson, W. R.; Rakitzis, T. P.; Kandel, S. A.; Orr-Ewing, A. J.; Zare, R.N. *J. Phys. Chem*. **1996**, *100*, 7938.
(44) Zhou, J.; Zhang, J. J.; Liu, K. *Mol. Phys*. **2005**, *103*, 1757.